Int. J. Heat Mass Transfer. Vol. 35, No. 11, pp. 2921–2929, 1992
Printed in Great Britain

0017–9310/92 $5.00+0.00
© 1992 Pergamon Press Ltd

Experimental studies on the dynamics and evaporation of tandem liquid droplets in a hot gas flow

K. J. CHOI† and H. J. LEE‡

Department of Mechanical Engineering, University of Illinois at Chicago, Chicago, IL 60680, U.S.A.

(*Received* 5 *November* 1990 *and in final form* 2 *December* 1991)

Abstract—Dynamics and evaporation of tandem droplets moving upward in a free convective thermal boundary layer were experimentally investigated. The free convective boundary layer was formed from a hot isothermal vertical plate which has a high wall-to-ambient temperature difference. The gas velocity and temperature profiles were numerically obtained using the variable gas property model, and the results were used to analyze the droplet dynamic behavior and vaporization process. The effects of droplet interaction in the streamwise direction and mass transfer on the drag coefficient were studied. In addition, the effects of droplet dynamics on droplet evaporation were investigated. The experimental parameters tested in this study were the initial droplet size, spacing between droplets, and liquid properties. New drag coefficients for various liquids and droplet spacings were obtained and applied to the vaporization process.

INTRODUCTION

KNOWLEDGE of dynamics and thermal behaviors of evaporating droplets in a hot gas stream is of great importance in the analysis of engineering problems involving a liquid spray. Some examples of this type of spray system are spray combustion, nuclear reactor emergency cooling, and compact droplet heat exchangers.

When liquid droplets are suddenly exposed to a hot environment, initially the temperature of the droplet rises rapidly, and is then followed by thermal processes, such as evaporation and/or combustion. The thermal behaviors of liquid sprays in a confined geometry depend significantly on droplet dynamics, while the droplet dynamics are affected by the mass transfer phenomena of evaporation. In addition, in an actual spray system the droplets interact and momentum and heat transfer behaviors are in an unsteady-state. Therefore, the droplet dynamics and thermal behaviors are also influenced by the droplet interactions and unsteady-state nature. All these factors contribute to the complexity of dynamic and thermal behaviors of evaporating spray droplets.

In the past, intensive studies on droplet dynamics of single non-evaporating droplets or particles have been conducted [1], and the information has frequently been applied to the studies of evaporating single droplets and spray [2]. However, the information of single non-evaporating droplet transport phenomena cannot be applied with any assurance of accuracy to an evaporating spray system due to the various effects mentioned above. Some studies were directed toward understanding one or more of these effects on droplet dynamics and evaporation. Eisenklam *et al.* [3] and Yuen and Chen [4] measured drag coefficients experimentally for evaporating and/or burning single droplets of various fuels. Their experimental data were found to be in good agreement with non-evaporating solid sphere drag coefficients, the so-called 'standard drag' curve, in the range of Reynolds number from 1 to 2000. However, their experiments were conducted with free-falling single droplets so that the nature of momentum transfer was a quasi-steady state. The unsteady momentum transfer effect was experimentally investigated by Briffa [5] using a water spray decelerating in an airstream. The analysis of the dynamic data for unsteady momentum transfer revealed that the drag coefficients were much different from the 'standard drag' curve. Recently, Dwyer and Sanders [6] conducted a numerical analysis for the drag coefficients of unsteady evaporating single droplets. Their results showed that the drag coefficients significantly differ from those of non-evaporating steady-state. The disagreement between the theoretical analysis and previous experimental results is explained by the unsteady momentum transfer through vaporization. As mentioned earlier, consideration of droplet interaction is also of great importance in the analysis of droplet dynamics, as well as the thermal behaviors of a liquid spray. Previous theoretical studies on droplet interactions have considered droplets in arrays or clouds in the absence of forced convection (the diffusion theory) [7, 8]. Calculations of this type indicated that interactions can significantly reduce droplet evaporation rates, even for large spacings between droplets. Shuen [9] has studied numerically the effects of droplet interactions on drag and evaporation of a planar droplet array in a steady-state situation under the presence of forced

† Present address: Department of Mechanical Engineering and Mechanics, Drexel University, Philadelphia, PA 19104, U.S.A.

‡ Present address: Department of Mechanical Engineering, Kangwon National University, Chuncheon, Kangwon-Do, Korea.

NOMENCLATURE

a	acceleration
B	mass transfer number
C_d	drag coefficient defined in equation (3)
c_p	specific heat at constant pressure
D	diameter
g	gravitational acceleration
H	gap distance between a tandem droplet stream and a hot plate
h	heat transfer coefficient
k	thermal conductivity
L	spacing distance between droplets in axial direction
Nu	Nusselt number, hD_d/k
Pr	Prandtl number, α/ν
Re	Reynolds number defined in equation (5)
S	droplet spacing ratio to droplet diameter, L/D
T	temperature
t	time
U	velocity component in the x direction
x	coordinate in heater plate axial direction
y	coodinate normal to the heater plate.

Greek symbols

α	thermal diffusivity, $k/\rho c_p$
ν	kinematic viscosity
ρ	density.

Subscripts

0	at initial condition
d	droplet
g	gas
l	liquid
r	at reference condition according to 1/3 rule
w	heater surface.

convection. Recent studies [10, 11] also revealed that droplet interactions have a significant role in both droplet dynamics and droplet evaporation.

Up to now, there has been little attempt to study the collaborative effects of mass transfer, unsteady-state momentum transport, and droplet interactions on both droplet dynamics and evaporation due to the complexity of experimental and analytical studies. Therefore, in this study, we have attempted to investigate the dynamic and thermal behaviors of liquid droplets where the droplets were under the influences of mass transfer, unsteady-state momentum transport, and droplet interaction. In order for the experimental and analytical tasks to be feasible and practical, a laminar free convective gaseous flow was selected in which tandem liquid droplets were injected. The laminar hot gas flow was produced by natural convection from a vertical isothermal plate. A single stream of mono-sized droplets was injected inside the laminar free convective flow adjacent to a vertical isothermal plate. The advantage of this system is that the analysis of the flow field and experimental measurements of droplet dynamics and evaporation are fairly easy. In addition, the control of the gas field and droplet characteristics (i.e. initial droplet size and droplet spacing) is relatively simple, and yet all the essential physics of the involved problem are retained.

EXPERIMENTAL APPARATUS AND PROCEDURES

This experimental investigation was aimed at characterizing such effects as mass transfer, the unsteady-state nature, and droplet interaction in a tandem stream moving in a hot gas medium on droplet dynamics and thermal behaviors. For this purpose, a simple but systematic experimental system was employed. As shown in Fig. 1, the experimental apparatus consisted mainly of two parts, i.e. a vertical hot plate for a laminar free gas boundary layer and a tandem droplet generating system. Although most droplet transport phenomena in an actual spray system take place in a forced convection situation, a system of droplets moving in a laminar free gas boundary layer has been adopted in this study for experimental simplicity.

A 0.15×1.6 m copper plate of 0.32 cm thickness was clamped over two electric heaters (800 W each). The outer surface of the copper plate was chrome-plated with 5 μm thickness to prevent oxidization. The heating power of two electric heaters beneath the copper plate was independently controlled so that the surface temperature of the hot plate could be maintained as uniform as possible. Two stainless-steel, sheathed, and ungrounded chromel–alumel (type K) thermocouples of 0.05 cm diameter were press fitted halfway into the thickness of the copper plate through the back surface of the heating plate. In order to minimize heat loss from the heating plate, the back surface of the heater was well insulated with fiberglass material. The vertical heating plate was supported with a precision translator so that the movement of the heating plate both forwards and backwards with respect to a reference position could be specifically measured. The precise movement of the heating plate was necessary because the gap distance between the stream of droplets and the vertical hot plate had to be controlled.

Mono-sized tandem droplets, with variable droplet spacing, were produced using both an impulse-jet droplet generator and a droplet selecting device, as shown in Fig. 1. Both devices were developed in our

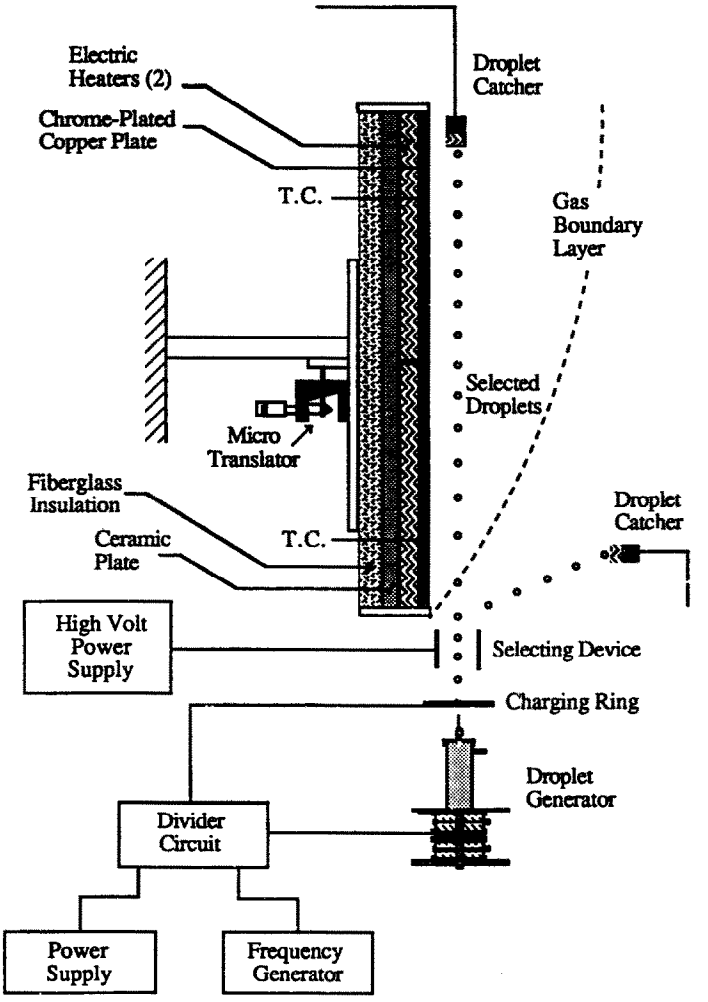

FIG. 1. Schematic of experimental set-up.

spray laboratory and a detailed description has been presented in the literature [12]. Therefore, only a brief description is given here. The impulse-jet droplet generator was originally developed for use in the ink-jet printer industry [13]. The basic principle of the device uses the impulse force generated from piezoelectric transducers in order to break a liquid jet into small uniform-sized droplets. In our device, the available maximum impulse force was obtained by using a vibrating piston positioned above a cylindrical liquid chamber. Four annular disk type piezoelectric transducers vibrated the piston at the optimum electric frequency. The liquid jet was then broken into monosized small droplets. The size of the droplets was controlled by varying the hypodermic needle size and applied electric signal frequencies. Since the droplet spacing to droplet diameter ratio for the tandem droplets generated with this impulse-jet droplet generator was very small (i.e. $S < 5$) and varied in a narrow range, a droplet-selecting device was necessary to increase the spacing. The droplet-selecting device consisted of a charging ring 1 cm in diameter and a set of two deflection plates. Electric potentials ranging from 150 to 300 V were applied to the charging ring at a certain frequency which could be varied by a frequency division circuit. The frequency division circuit was driven at the same frequency as the impulse-jet generator; therefore, the frequency at which droplets were charged could be controlled. A constant potential of about 2200 V was applied to the deflection plates in order to deflect the charged droplets from a stream of monosized droplets. The uncharged droplets were not deflected and remained in the original droplet path. The capability of droplet removal from the stream of droplets enabled control of droplet spacing. The experimental conditions used in this study are summarized in Table 1.

A stream of mono-sized droplets at a fixed droplet spacing was injected from the lower portion of the experimental set-up parallel to the vertical plate. The spacing between the stream of droplets and the plate was carefully set by using a precision translator (with 1/100 mm accuracy). The vertical trajectory of droplets was checked using a microscopic camera at vari-

Table 1. Summary of experimental conditions used in this study

Liquid	D_d (μm)	S	T_w (K)	H (mm)
Water	290, 645	4, 53	811	1, 3
Methanol	330, 637	2.8, 3.7	811	1, 3
Ethanol	255, 285	48, 51	811	1, 3
Hexane	410	2.1, 3.4	811	1, 3

ous locations so that the stream of droplets was accurately aligned to be parallel to the plate. A droplet-catcher was positioned at the upper portion of the test section so that the droplets were collected not to fall back down and the natural convection plumes in the middle region of the test section would not be interfered with by the droplet-catcher. The vertical heating plate was then heated to 550°C while the two electric heaters embedded in the vertical plate were independently controlled to be uniform in temperature. The droplet size and droplet spacing were measured using a polaroid microscopic camera at various plate axial locations. The velocity of widely spaced tandem droplets was measured using a double-image technique with a 200 mm zoom camera and a strobe light. The camera shutter speed and the time interval of the strobe light were 1/1000 and 1/2000 s, respectively. However, the velocity of closely spaced tandem droplets was measured using a single-image photograph taken with a polaroid microscopic camera. With the assumption of no coalescence or breaking-up of droplets, the droplet spacing and the droplet number rate were used to calculate the individual droplet velocity as follows:

$$U_d \cong Lf \tag{1}$$

where f is the number of droplets per unit time, calculated from the electric frequencies used for the impulse-jet droplet generator and the droplet selection divider. The validity of this method was proved by comparison of the two different methods mentioned above. Figure 2 shows sample photographs of hexane tandem droplets at $x = 0$ cm and $x = 10.5$ cm, respectively, in a hot gas convective flow. The initial droplet size, spacing-to-diameter ratio, spacing between the hot plate and the droplet stream, and the plate wall temperature used for this test are 408 μm, 3.2, 1 mm, and 811 K, respectively. Since the hot surface was chrome-plated and mirror finished, the image of tandem droplets was reflected onto the hot surface as shown in Fig. 2.

ANALYSIS OF EXPERIMENTAL DATA

The droplet sizes and velocities measured from photographs were curve fitted to the first order least square along the plate axial distance, x. The acceleration rate of the droplet was then calculated from the velocity profile with the axial distance as follows:

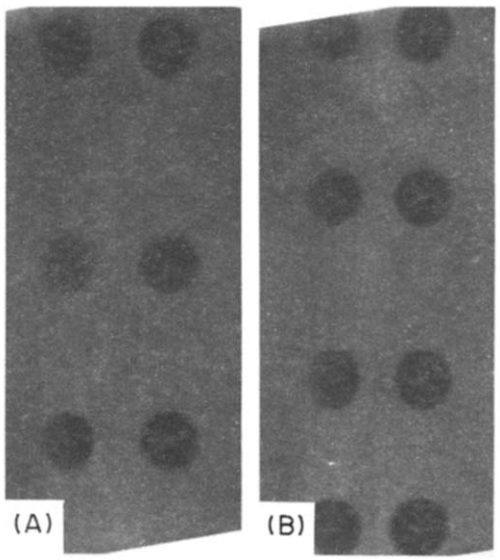

Fig. 2. Sample photos of tandem water droplets in a laminar free convective flow: (A) at $x = 0$ cm, (B) at $x = 10$ cm.

$$a_d = \frac{dU_d}{dt} = \frac{1}{2}\frac{dU_d^2}{dx}. \tag{2}$$

From the conservation of momentum, a relationship between the droplet acceleration a_d and the drag coefficient C_d was obtained as follows:

$$C_d = \frac{4}{3}\frac{\left(\frac{1}{2}\frac{dU_d^2}{dx} + g\right)D_d}{|U_g - U_d|(U_g - U_d)}\frac{\rho_l}{\rho_g}. \tag{3}$$

As shown in equation (3), the drag coefficient is a function of the droplet acceleration rate, droplet size, and relative velocity of droplet to gas flow. The gas velocity profile could be determined by solving the laminar free boundary layer equations for a vertical isothermal plate with high surface-to-ambient temperature difference. Due to the high surface-to-ambient temperature difference, the variable fluid property approach was employed. Sun [14] has solved this problem numerically and the same method has been adopted in this paper. Although the gas flow fields might be interfered with by the moving tandem droplets, for simplicity of data analysis, no interference in the gas flow fields by the droplet motion was assumed.

The gas properties, namely, viscosity, density, and thermal conductivity, were obtained at the droplet reference temperature, defined as [15]

$$T_r = T_d + (T_g - T_d)/3. \tag{4}$$

The droplet Reynolds number is defined as

$$Re_d = \frac{D_d|U_g - U_d|}{\nu_{g,r}}. \tag{5}$$

RESULTS AND DISCUSSION

Gas phase

In order to experimentally analyze the droplet dynamics and vaporization phenomena, gas phase

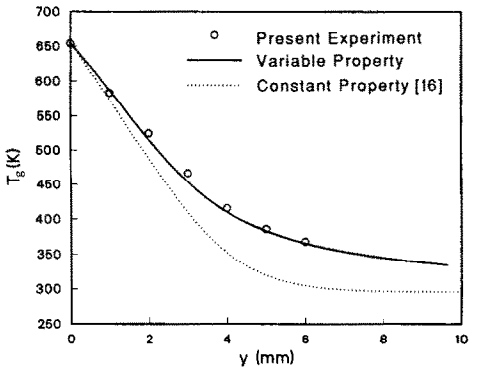

FIG. 3. Comparison of experimental and theoretical gas-phase temperature profiles.

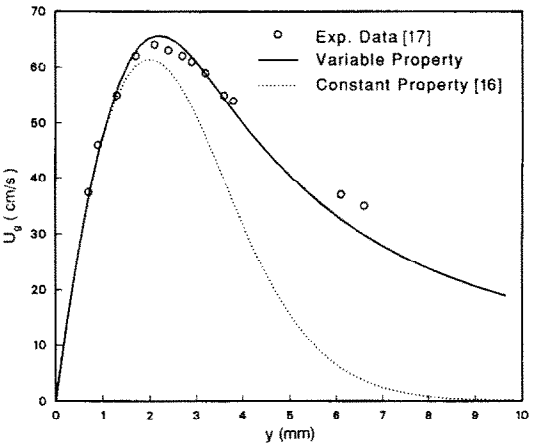

FIG. 4. Comparison of experimental and theoretical gas-phase velocity profiles.

properties such as temperature and velocity at each droplet location had to be pre-determined. Therefore, theoretical calculation of the fluid temperature and velocity profiles was conducted.

Figure 3 shows the theoretical result of the gas phase temperature profile, together with the corresponding experimental result. The theoretical analysis does not account for droplet existence in the gas phase, while the experiment was based upon having a stream of water droplets injected into the hot gas. For the experimental results, the gas temperature was measured with a 0.05 cm diameter thermocouple probe at various transverse locations from the hot plate with the axial distance from the bottom of the plate fixed at $x = 10$ cm. Due to interaction of droplets with the gas flow, the gas temperature fluctuated somewhat. For the fluctuating case, several measurements at each fixed location were averaged and plotted in Fig. 3. As shown in Fig. 3, the experimental and theoretical results are in good agreement. Ostrach's solution [16] of the constant gas property problem is also shown for comparison. This result demonstrates clearly that the constant property theory does not give an adequate representation of the gas temperature field for a high plate-to-ambient temperature difference. Throughout this study, the variable gas property theory was adopted to determine both the gas temperature and velocity profiles.

The gas velocity profile along the y-axis at $x = 10$ cm is presented in Fig. 4 in dimensional form. The measurement of gas velocity was not attempted in this study. Instead, Cairnie and Harrison's [17] experimental results under equivalent conditions are used to verify present theoretical results. As shown in Fig. 4, the result of the variable gas property theory is in good agreement with the experimental measurement.

Droplet dynamics

For the experimental study of droplet dynamics, droplet velocities at various locations along the hot plate axial distance (x) were measured using photographs, as shown in Fig. 2. As the droplets move upward, the droplet velocity decreases due to gravity and drag, while the droplet size decreases through the vaporization process.

Figure 5 shows the droplet velocity profile for methanol tandem droplets of 630 μm initial diameter. For this test, the initial droplet velocity, the hot plate surface temperature, the initial droplet spacing ratio, and the gap distance between the droplets and the hot wall were 318 cm s^{-1}, 811 K, 3.4, and 1 mm, respectively. As shown in Fig. 5, the data points are scattered due to droplet oscillation in the hot air streams. Therefore, the data points were curve fitted using a first order linear regression method. The correlation fits the data within $\pm 5\%$.

Using equations (2)–(5), the droplet drag coefficient and the Reynolds number at each axial location were calculated. For the calculation, information of the droplet size variation with the axial distance (see Fig. 7) was utilized. The drag coefficient profiles with Reynolds numbers are plotted in Fig. 6 for various liquid droplets under different initial droplet conditions. Along with the present experimental results, the so-called 'standard curve' for a single, steady-state, and non-evaporating sphere is presented. It should be noted here that the error bound of the drag coefficients may be greater than that of the drop-

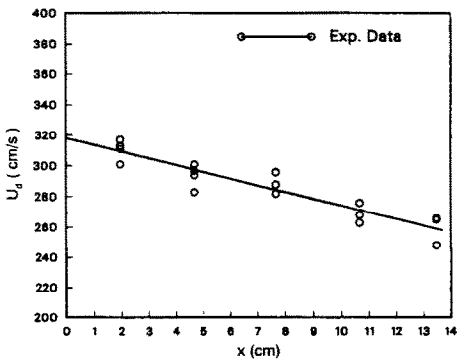

FIG. 5. Velocity profile of closely spaced methanol droplets along the hot plate axial distance; $S = 3.4$, $H = 1$ mm, $D_{d,0} = 640$ μm, and $T_w = 811$ K.

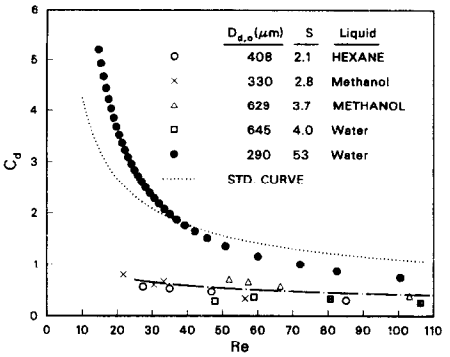

FIG. 6. Drag coefficient profiles with Reynolds number for various liquids and droplet spacings.

let velocities, because the drag coefficients presented in equation (3) are calculated from the curve-fitted droplet velocity profiles. The accuracy of the drag coefficient results, therefore, were examined by employing the maximum and minimum slopes of the curve-fitted velocity profile. Since the initial droplet velocity (i.e. at $x = 0$ cm) was known as a fixed value, the maximum error always occurs at the farthest location in the axial direction (i.e. at $x = 14$ cm). For the case of Fig. 5, the error bounds are $\pm 7\%$ and $\pm 15\%$ at $x = 0$ cm and $x = 14$ cm, respectively.

As shown in Fig. 6, when the initial droplet spacing ratio is less than 4, the drag coefficient profiles are collaboratively fitted to the following empirical equation:

$$C_d = 2.3\, Re_d^{-0.37} \tag{6}$$

in a Reynolds number range of 20–110. For closely spaced tandem droplets, i.e. $S < 4$, it was found that the vaporization rate or mass transfer from droplets was relatively small (this will be further discussed later), resulting in a negligible effect of mass transfer on the drag coefficient. Therefore, the major discrepancy in the drag coefficient between the standard curve and the empirical curve for closely spaced tandem droplets mainly resulted from the droplet interaction and/or unsteady-state nature of the droplet motion.

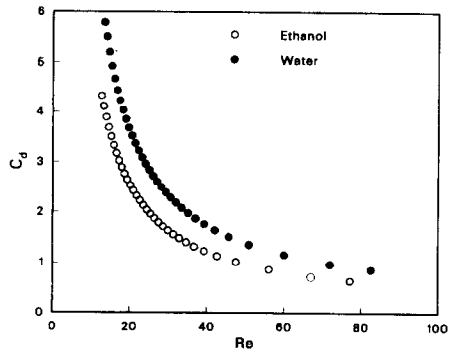

FIG. 7. Comparison of water and ethanol tandem droplet drag coefficient profiles; $H = 3$ mm and $T_w = 811$ K.

Figure 6 also shows the result for a widely spaced ($S = 53$) water droplet drag coefficient profile. Comparing this to the result of closely spaced tandem droplets, the spacing effect on the drag is apparent, i.e. the drag coefficients of closely spaced tandem droplets are much smaller than those of widely spaced droplets. This is due to the wake generated by the forefront droplet in a tandem droplet stream. The pressure drag on a droplet is significantly reduced when the droplet is in the wake of another droplet. Mulholland *et al.* [18] also claimed that droplet spacing had a dominant effect on the drag coefficient for tandem non-evaporating droplets.

A comparison of drag coefficients for widely spaced tandem droplets with the standard drag curve is presented in Fig. 6. It is observed that the drag coefficients of widely spaced water droplets are smaller than the standard drag values for a Reynolds number greater than 35. As mentioned before, the present experimental work has been conducted in unsteady-state conditions, i.e. the droplet was injected into a non-uniform gas medium against gravity, while the 'standard drag' curve was obtained at a steady-state condition. Recent studies on the transient drag of liquid droplets, i.e. deceleration or acceleration of droplets, indicated a large discrepancy in drag coefficients between transient and steady-state cases. Briffa [5] reported that the effects of deceleration of droplets typically lead to a lower drag coefficient compared to the steady-state value. In the present study, the liquid droplets were situated in a deceleration nature from the beginning. In addition, the environmental gas medium had non-uniform properties; that is, the gas velocities and temperatures varied with the axial distance. When a droplet is injected into the gas medium the droplet velocity rapidly decelerates due to gravity and drag. This deceleration effect causes a reduced drag coefficient in the Reynolds number range from 35 to 110, as shown in Fig. 6. However, as the droplet moves further upward, the increased gas velocity begins to have a significant effect on the droplet dynamics. As a result, the deceleration rate of the droplet decreases, and the drag coefficient approaches the standard value. Eventually, the trend becomes reversed, i.e. the drag coefficient is greater than the standard value. This is shown in Fig. 6 for a Reynolds number less than 35. The unsteadiness of the droplet motion coupled with the non-uniform behavior of fluid motion results in the present drag coefficients.

The effect of mass transfer on the droplet dynamics is shown in Fig. 7. Widely spaced tandem droplets ($S = 51$–53) of two different liquids, i.e. water and ethanol, were tested. The transient nature of the droplet motion and the effects of droplet interaction on the droplet motion are identical for the two liquids. Since vaporization of a water droplet during the short period of time at the heater temperature used was not appreciable, the effect of mass transfer on the droplet dynamics was negligible. However, for an ethanol droplet, evaporation must be considered. As shown

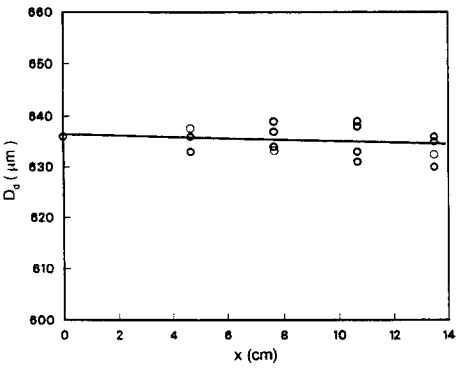

FIG. 8. Changing droplet diameters with axial distance for closely spaced methanol tandem droplets; $S = 2.9$, $H = 1$ mm, and $T_w = 811$ K.

in Fig. 7, the drag coefficient for the ethanol droplet is slightly lower than for the water droplet in the Reynolds number range tested. Although this report shows the effect of evaporation on the drag coefficient, it is only a first experimental case which requires further experiments to verify and analyze the above observation.

Droplet evaporation

As liquid droplets move upward in a hot gas flow, the droplets are heated and vaporized by convection and radiation heat transfer. The droplet size variation along the axial distance of the plate for closely spaced ($S = 2.9$) methanol tandem droplets is plotted in Fig. 8. The heater surface temperature and the gap distance H are the same as in Figs. 5–7. In order to eliminate droplet-size irregularities, the data were curve-fitted by first order linear regression. The droplet stream had a very small spacing ratio, necessitating a long heating time for the droplets with little vaporization taking place. The cold boundary surrounding each droplet was formed by its forefront droplet, resulting in the prevention of hot gas from penetrating the droplet. Due to the deceleration process as the droplet moves upward, the droplet spacing becomes closer and vaporization becomes more difficult. Changes in droplet size for widely spaced tandem droplets ($S = 48$) are shown in Fig. 9, using ethanol droplets of 255 μm initial diameter. Comparing with the case shown in Fig. 8, much more evaporation occurred due to higher heat transfer to the single isolated-type droplet.

In order to compare the present experimental result with theoretical analysis, a theoretical computation was performed using the infinite conduction limit model for the droplet vaporization process [14]. The present authors, however, modified the theoretical model by employing the experimental result for the drag coefficients of the widely spaced tandem droplets (e.g. Fig. 6). For most single isolated droplets, the following Ranz–Marshall correlation [19] was used for heat transfer to the droplet:

$$Nu = 2.0 + 0.6\, Pr^{1/3}\, Re_d^{1/2}. \tag{7}$$

The change of droplet size is also given by the Ranz–Marshall correlation as follows:

$$\frac{dD_d^2}{dt} = -\frac{8\rho_g \mathscr{D}}{\rho_l}(1 + 0.3\, Re_d^{1/2}) \ln(1+B) \tag{8}$$

where $\mathscr{D}$ and B are the mass diffusivity and Spalding transfer number, respectively. As shown in Fig. 9, the theoretical calculation shows less vaporization through the droplet motion up to $x = 15$ cm than the experimental measurement. The discrepancy between the theoretical and experimental results could have resulted from the vaporization model used in this study, i.e. the infinite conductivity limit model. The infinite conductivity limit model does not appear to accurately represent the current vaporization process. Further study should try to utilize other potential analytical models of droplet vaporization such as the conduction limit and vortex models [20].

When spray vaporization is considered, existing analytical models should be applied carefully due to the various factors mentioned previously, such as droplet interaction and the unsteady-state nature of droplet motion. In order to see the importance of these factors, theoretical and experimental results of droplet vaporization for a closely spaced droplet stream are

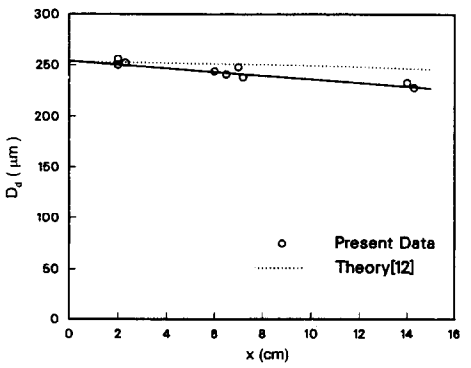

FIG. 9. Comparison of experimental and theoretical results of change in droplet size for widely spaced ethanol droplets; $S = 48$, $H = 3$ mm, and $T_w = 811$ K.

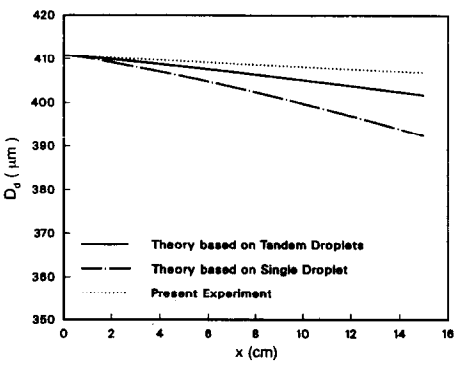

FIG. 10. Comparison of experimental and theoretical results of change in droplet size for closely spaced n-hexane tandem droplets; $S = 3.4$, $H = 1$ mm, and $T_w = 811$ K.

compared in Fig. 10. For the analysis, typical hexane tandem droplets of $S = 3.4$, $H = 1$ mm, and $T_w = 811$ K were selected. For the theoretical calculation, two different approaches were conducted: (1) by assuming the tandem droplets as steady single isolated droplets and (2) by considering the factors influencing the droplet in a tandem droplet stream. The first case of theoretical calculation was, therefore, performed using equations (7) and (8) and the standard drag coefficient for a single steady non-evaporating droplet. However, for the second case of theoretical calculation, the heat transfer rate to the droplet had to be modified due to droplet interaction. Recently, Tong and Chen [21] numerically analyzed heat transfer for vaporizing liquid droplets in an array. They correlated the heat transfer rate with non-dimensional parameters for each droplet spacing ratio as follows:

$$Nu = 2.477\,(Re)^{0.206}(b/a)^{-0.191}(1+B)^{-0.601} \quad (9)$$

where the constants a and b are determined based on droplet spacing ratios ranging from 1.5 to 4.0. Therefore, for the second type of theoretical calculation of closely spaced tandem droplet vaporization, equation (9) and the drag coefficient for the tandem unsteady droplets, as given in Fig. 6, were used. Comparing the two theoretical results, it is noted that the theoretical calculation of the vaporization rate with consideration of droplet interaction is in better agreement with the experimental results. However, the theoretical calculation with consideration of droplet interaction even overestimates the vaporization rate, which is contradictory to the case of widely spaced ethanol droplets (see Fig. 9). The reason is that for the closely spaced case the gas flow fields are interfered with by the stream of droplets.

Therefore, in order to accurately predict the vaporization rate for closely spaced droplets moving in natural convection plumes, it is necessary to consider interaction of gas flow fields with droplets as well as interaction between droplets.

CONCLUSIONS

Dynamics and evaporation of tandem droplets moving upward in a free convective thermal boundary layer were investigated experimentally. The effects of droplet interaction in the stream direction and mass transfer on the drag coefficient were tested. The drag effect on droplet evaporation was also studied. The results are summarized as follows:

(1) The laminar free convective flow from a vertical isothermal plate with high wall-to-ambient temperature difference can be solved with the variable gas property theory. The numerical results based on the variable property model are in good agreement with experimental results.

(2) Droplet interaction of closely spaced tandem droplets has a significant effect on the drag coefficient, i.e. closely spaced tandem droplets ($S \leqslant 4.0$) have a much lower drag coefficient than widely spaced droplets ($S > 50$).

(3) Unsteadiness in droplet–gas relative motion has a significant effect on the drag coefficient, i.e. during a severe deceleration process due to gravity and drag the drag coefficient is much lower than the steady-state case; however, when the deceleration rate reduces rapidly due to increased gas velocity, the trend is reversed.

(4) Vaporization of a single isolated-type droplet reduces the drag coefficient, compared to the non-vaporizing droplet case.

(5) The droplet interaction significantly affects the vaporization process of closely spaced tandem droplets. Therefore, accurate values of drag coefficient and heat transfer should be applied for calculation of the droplet evaporation rate in a confined geometry.

Acknowledgements—This research was supported by the National Science Foundation and the University of Illinois at Chicago. The authors also wish to acknowledge Mr Tim Serges at UIC for the experiment.

REFERENCES

1. R. Clift, T. R. Grace and M. E. Weber, *Bubbles, Drops, and Particles*. Academic Press, New York (1978).
2. C. K. Law, Recent advances in droplet vaporization and combustion, *Prog. Energy Combust. Sci.* **8**, 171 (1982).
3. P. Eisenklam, S. A. Arunachalan and J. A. Weston, Evaporation rates and drag resistance of burning drops, *11th Int. Symp. on Combustion*, pp. 715–727 (1967).
4. M. C. Yuen and L. W. Chen, On drag of evaporating liquid droplets, *Combust. Sci. Technol.* **14**, 147–154 (1976).
5. F. E. J. Briffa, Transient drag in sprays, *18th Symp. (Int.) on Combustion*, The Combustion Institute, pp. 307–319 (1981).
6. H. A. Dwyer and B. R. Sanders, Detailed computation of unsteady droplet dynamics, *20th Int. Symp. on Combustion*, pp. 1743–1749 (1984).
7. M. Labowski, Calculation of the burning rates of interacting fuel droplets, *Combust. Sci. Technol.* **22**, 217–226 (1980).
8. M. Marberry, A. K. Ray and K. Leung, Effect of multiple particle interactions on burning droplets, *Combust. Flame* **57**, 237–245 (September 1984).
9. J.-S. Shuen, Effects of droplet interactions on droplet transport at intermediate Reynolds numbers, AIAA 25th Aerospace Sciences Meeting, AIAA-87-0137 (1987).
10. Q.-V. Nguyen, R. H. Rangel and D. Dunn-Rankin, Measurement and prediction of trajectories and collision of droplets, *Int. J. Multiphase Flow* **17**, 159–177 (1991).
11. C.-H. Chiang and W. A. Sirignano, Numerical analysis of convecting and interacting vaporizing fuel droplets with variable properties, presented at the 28th AIAA Aerospace Sciences Meeting, Reno, Nevada (1990).
12. K.-J. Choi and B. Delcorio, Generation of controllable mono-dispersed sprays using impulse jet and charging techniques, *Rev. Sci. Instrum.* **61**, 1689–1693 (1990).
13. J. Heinzl and C. H. Hertz, Ink-jet printing. In *Advances in Electronics and Electron Physics*, Vol. 65, pp. 91–171. Academic Press, New York (1985).
14. Z. Sun, Vaporization and auto-ignition characteristics of liquid droplets adjacent to a vertical hot plate, M.S. Thesis, University of Illinois at Chicago (1988).

15. M. C. Yuen and L. W. Chen, Heat transfer measurements of evaporating liquid droplets, *Int. J. Heat Mass Transfer* **21,** 537–452 (1978).
16. S. Ostrach, Analysis of laminar free convective flow and heat transfer about a flat plate parallel to the direction of generating body force, NACA Technical Note 2635 (1952).
17. L. R. Cairnie and A. J. Harrison, Natural convection adjacent to a vertical isothermal hot plate with a high surface-to-ambient temperature difference, *Int. J. Heat Mass Transfer* **25,** 925–934 (1982).
18. J. A. Mulholland, R. K. Srivastava and J. O. L. Wendt, Influence of droplet spacing on drag coefficient in non-evaporating, monodisperse streams, *AIAA J.* **26,** 1231–1237 (1988).
19. W. E. Ranz and W. R. Marshall, Evaporation from drops—Part 2, *Chem. Engng Prog.* **48,** 173–180 (1952).
20. S. K. Aggarwal, A. Y. Tong and W. A. Sirignano, A comparison of vaporization models in spray calculations, *AIAA J.* **22,** 1448–1457 (1984).
21. A. Y. Tong and S. J. Chen, Heat transfer correlations for vaporizing liquid droplet arrays in a high-temperature gas at intermediate Reynolds number, *Int. J. Heat Fluid Flow* **9,** 118–130 (1988).

ETUDES EXPERIMENTALES DE LA DYNAMIQUE ET DE L'EVAPORATION DE GOUTTELETTES LIQUIDES EN TANDEM DANS UN ECOULEMENT DE GAZ CHAUD

Résumé—On étudie expérimentalement la dynamique et l'évaporation de gouttelettes se déplaçant vers le haut l'une derrière l'autre dans une couche limite thermique de convection naturelle. Celle-ci est formée par une plaque verticale isotherme chaude avec une différence de température élevée par rapport à l'ambiance. Les profils de vitesse et de température du gaz sont obtenus numériquement par un modèle avec propriétés variables du gaz, et les résultats sont utilisés pour analyser le comportement dynamique des gouttelettes et le mécanisme de vaporisation. Les effets d'interaction des gouttes dans la direction du mouvement et du transfert de masse sur le coefficient de trainée sont étudiés. De plus, on étudie les effets de la dynamique des gouttelettes sur l'évaporation. Les paramètres expérimentaux testés sont la taille initiale des gouttelettes, l'espacement entre elles et les propriétés du liquide. Des nouveaux coefficients de trainée pour différents liquides et espacements sont obtenus et appliequés au mécanisme de vaporisation.

EXPERIMENTELLE UNTERSUCHUNG DER DYNAMIK UND DER VERDAMPFUNG VON FLÜSSIGEN DOPPELTROPFEN IN EINEM HEISSEN GASSTROM

Zusammenfassung—Die Dynamik und die Verdampfung von Doppeltropfen, welche in einer thermischen Grenzschicht bei freier Konvektion aufwärts strömen, werden experimentell untersucht. Die Grenzschicht bei freier Konvektion bildet sich an einer isothermen senkrechten Platte großer Temperaturdifferenz zwischen Wandoberfläche und Umgebung. Unter Verwendung eines Modells mit variablen Stoffeigenschaften des Gases werden numerisch die Geschwindigkeit und Temperaturprofile ermittelt. Die Ergebnisse dienen dazu, das dynamische Verhalten und den Verdampfungsvorgang der Tropfen zu untersuchen. Insbesondere werden die Einflüsse der Wechselwirkung zwischen den Tropfen in Strömungsrichtung und des Stoffübergangs auf den Strömungswiderstand untersucht. Von Interesse ist außerdem der Einfluß der Tropfendynamik auf die Verdampfung. Der Einfluß folgender Versuchsparameter wird untersucht: anfängliche Tropfengröße, Abstand zwischen den Tropfen und Eigenschaften der Flüssigkeit. Für die unterschiedlichen Flüssigkeiten und Tropfenabstände werden neue Widerstandskoeffizienten ermittelt und auf den Verdampfungsvorgang angewandt.

ЭКСПЕРИМЕНТАЛЬНОЕ ИССЛЕДОВАНИЕ ДИНАМИКИ И ИСПАРЕНИЯ КАПЕЛЬ ЖИДКОСТИ В ПОТОКЕ НАГРЕТОГО ГАЗА

Аннотация—Экспериментально исследовались динамика и испарение двойных капель, движущихся вверх в свободноконвективном тепловом пограничном слое, образовавшемся на нагретой изотермической пластине с высокой разностью температур стенки и окружающей среды. С использованием модели переменных свойств газа численно определены профили скоростей и температур газа, и полученные результаты использованы для анализа динамических характеристик капель и процесса парообразования. Исследовалось влияние взаимодействия капель в направлении течения, а также массопереноса на коэффициент сопротивления. Кроме того, определялось влияние динамики капель на их испарение. Экспериментально определялись такие параметры как начальный размер капель, расстояние между ними и свойства жидкости. Найдены коэффициенты сопротивления для различных жидкостей и расстояний между каплями, значения которых использованы при исследовании процесса парообразования.